

Anomalous Magnetic Ground State in an LaAlO₃/SrTiO₃ Interface Probed by Transport through Nanowires

A. Ron,¹ E. Maniv,¹ D. Graf,² J.-H. Park,² and Y. Dagan^{1,*}

¹Raymond and Beverly Sackler School of Physics and Astronomy, Tel-Aviv University, Tel Aviv, 69978, Israel

²National High Magnetic Field Laboratory, Florida State University, Tallahassee, Florida 32310, USA

(Received 6 January 2014; revised manuscript received 11 August 2014; published 17 November 2014)

Resistance as a function of temperature down to 20 mK and magnetic fields up to 18 T for various carrier concentrations is measured for nanowires made from the SrTiO₃/LaAlO₃ interface using a hard mask shadow deposition technique. The narrow width of the wires (of the order of 50 nm) allows us to separate out the magnetic effects from the dominant superconducting ones at low magnetic fields. At this regime hysteresis loops are observed along with the superconducting transition. From our data analysis, we find that the magnetic order probed by the giant magnetoresistance effect vanishes at $T_{\text{Curie}} = 954 \pm 20$ mK. This order is not a simple ferromagnetic state but consists of domains with opposite magnetization having a preferred in-plane orientation.

DOI: 10.1103/PhysRevLett.113.216801

PACS numbers: 73.63.-b, 74.78.Na, 75.70.Cn, 75.75.-c

The nature of the magnetic state at the interface between LaAlO₃ and SrTiO₃ and its coexistence with superconductivity has been at the focus of recent intense scientific research. Brinkman *et al.* found strong, sweep-rate-dependent hysteretic behavior of the magnetoresistance [1]. Additional transport experiments suggested magnetic order at high magnetic fields [2–4]. Transport in atomic force microscope written nanowires has been attributed to a spin based mechanism related to emergent magnetism [5]. Bert *et al.* [6] Dikin *et al.* [7], and Li *et al.* [8] suggested that superconductivity and ferromagnetism do coexist in the same temperature-magnetic field domain in the phase diagram but no evidence for spatial coexistence has been demonstrated. On the other hand, while torque magnetometry [8] suggested a strong magnetic moment per site, of the order of $0.3\mu_B$, with μ_B the Bohr magneton, the scanning SQUID experiment [6] and β NMR measurements [9] suggested weaker magnetization. X-ray magnetic circular dichroism and x-ray absorption spectroscopy suggested that unique magnetism resides on the titanium d_{xy} orbital [10]. Recently, we have shown that the conductance through a ballistic quantum wire has step height of e^2/h [11], indicative of removal of spin degeneracy.

On the theory side, a mechanism for the coexistence of superconductivity on the homogeneous background of localized magnetic moments has been suggested [12]. Banerjee *et al.* suggested a spiral order to reconcile the discrepancy between the various magnetization probes [13]. Ruhman *et al.* interpreted the magnetotransport properties as a competition between Kondo screening at high carrier concentration and magnetism for low carrier concentration [14].

Fabricating nanostructures out of the LaAlO₃/SrTiO₃ interface is challenging [15–17] since SrTiO₃ is prone to spurious conductivity generated by oxygen vacancies. We

have recently shown that the boundary between two non-conducting interfaces is a ballistic quantum wire [11]. Here we present a new method for fabricating nanowires. Measurements of such 50 nm wide wires exhibit Shubnikov–de Haas (SdH) oscillations at high magnetic fields of the order of 10 T. The small width of the wires allowed us to separate out the magnetic contributions to the resistance from the dominant superconductivity and to observe hysteresis effects below the superconducting critical field H_c . The shape of the hysteresis and its angular dependence suggest an anomalous magnetic ground state consisting of adjacent magnetic domains aligned antiparallel.

Epitaxial films of LaAlO₃ 10 unit cells thick are deposited using reflection high energy electron diffraction (RHEED) monitored pulsed laser deposition on atomically flat TiO₂ terminated SrTiO₃ (100) 0.5 mm thick substrates in standard conditions, oxygen partial pressure of 1×10^{-4} Torr, and temperature of 780 °C, as described in Ref. [2] followed by an annealing step at 400 °C and oxygen pressure of 200 mTorr for 1 h to minimize the contribution of oxygen vacancies to conductivity [18] and magnetism [19]. Prior to the deposition of LaAlO₃ the samples were patterned with a hard mask of an amorphous oxide defining $5 \mu\text{m} \times 50$ nm nanowires, as depicted in Fig. 1. The RHEED system was used to calibrate the deposition rate by performing a deposition at the above conditions on a large sample prior to that of the nanowires, after which a third RHEED monitored film is deposited to ensure that the calibration remained valid. A gold layer is evaporated as a backgate. Ti-Au contacts were evaporated after Ar ion milling of the contact area. We use a wire bonder to connect voltage and current leads to each Ti-Au contact to eliminate the resistance of the leads, without eliminating the resistance between the metal and the nanowires. All samples were cooled down in a ³He

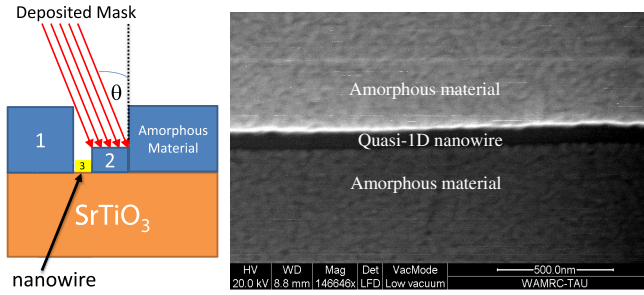


FIG. 1 (color online). Left: Fabrication method of the nanowires. On top of the TiO_2 terminated SrTiO_3 substrate an amorphous oxide layer number 1 with a thickness d was deposited and patterned with standard optical lithography process. The substrate is then tilted to an angle θ and a second amorphous oxide layer is deposited. This results in a nanotrench with a width $w = d \tan(\theta)$. Finally, an epitaxial LaAlO_3 layer is deposited as described in the text, resulting in a conducting $\text{LaAlO}_3/\text{SrTiO}_3$ nanowire. Right: Scanning electron microscope image of such a nanowire designed with $w = 70$ nm, consistent with the dimensions measured by the microscope.

refrigerator, and a few of them were also cooled down in a dilution refrigerator with a base temperature of 20 mK. Magnetic fields as high as 18 T were applied at various orientations. In the parallel orientation the field was either perpendicular to the current (transverse) or parallel to it (parallel). The presented sample resistances were measured using a Lakeshore 370 resistivity bridge with 3716 L low resistance preamplifier and scanner. In order to distinguish magnetic hysteresis effects intrinsic to the sample from the remanent field of the superconducting magnet, we also performed the measurements in a quenched magnet. In order to verify that the magnetic and superconducting phenomena observed are intrinsic to the samples, the zero and low field measurements were also reproduced in three different dilution refrigerators equipped with different lock-in amplifiers and applied currents between 0.1 and 5 nA. At least one of the measurement setups has been proven to show superconducting transition down to zero resistance in nanowires [20]. In this Letter we report data obtained from one sample; these data were reproduced in five other samples fabricated on two different substrates.

In Fig. 2(a) we show the resistance as function of temperature. Clearly a superconducting transition is observed; however, the resistance of the sample does not reach zero. This point will be addressed in the discussion. In Fig. 2(b) we show the resistance of the sample as a function of magnetic field applied perpendicular to the sample at 20 mK and $V_g = 0$ V (as grown state). Shubnikov-de Haas (SdH) oscillations are observed at perpendicular fields greater than 10 T, as shown in Fig. 2(c). We use this quantum effect to characterize our samples. According to Luttinger's theorem, the period of the SdH oscillations is directly related to the two-dimensional carrier density n_{2D} by $n_{2D} = eN_d F/h$, where N_d is the degeneracy. Ignoring

any degeneracy, the obtained frequencies [see fast Fourier transform in Fig. 2(d)] correspond to carrier densities of the order of 10^{12} cm^{-2} and can be modulated by application of gate voltage. These values are similar to those obtained for large samples [21].

In Fig. 2(e) the magnetoresistance at 20 mK for various gate voltages (going down from 31.2 to 22.8 V) is shown. The resistance, magnetoresistance, and superconducting properties are changing monotonically as reported for the 2D system in Ref. [22].

Figure 3 focuses on the low magnetic field dependence (up to ~ 200 G) at 20 mK for magnetic field applied perpendicular to the interface [Fig. 3(a)], transverse [Fig. 3(b)], and parallel to the wire [Fig. 3(c)]. As the field is swept back and forth (blue curves and red curves), a negative hysteretic magnetoresistance is observed. For perpendicular field orientation, subtraction of the superconducting background (see caption of Fig. 3) allows us a clearer observation of the magnetic effect. The curves are reproducible and their features are independent of field sweep rate (between the rates of 0.005 and 0.2 T/min).

The magnetic features are similar to the giant magnetoresistance (GMR) effect reported in granular ferromagnetic materials [23]. The presence of a similar magnetic feature

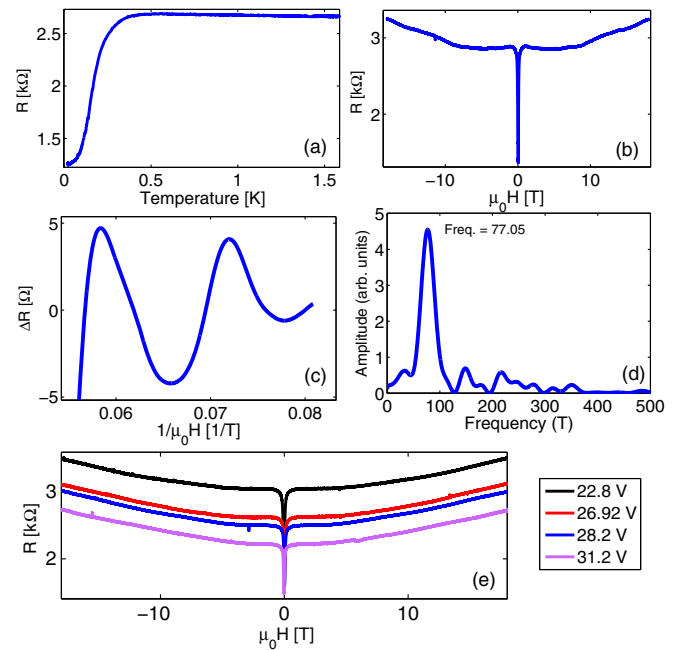


FIG. 2 (color online). (a) Resistance as function of temperature at zero magnetic field and $V_g = 0$ V (as grown). (b) Resistance as a function of magnetic field at 20 mK and $V_g = 0$ V (as grown). (c) Focus on the Shubnikov-de Haas (SdH) oscillations plotted as function of inverse field after application of a low pass filter to reduce measurement noise. Periodic oscillations are observed. (d) A fast Fourier transform of the SdH oscillations yielding a sharp peak at 77.05 T. (e) Resistance versus magnetic field for various gate voltages. The gate voltage is decreased from 31.2 (bottom magenta curve) to 22.8 V (top black curve)

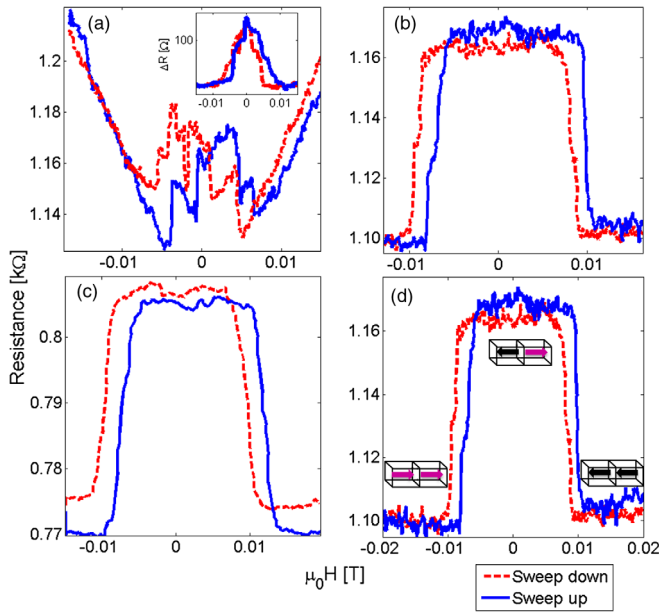


FIG. 3 (color online). Resistance as function of magnetic fields for the low fields region at 20 mK. Reproducible magnetic hysteresis curves are observed in (a) perpendicular, (b) transverse, and (c) parallel field orientations. Solid blue lines correspond to the curve plotted while increasing the field and the dashed red lines for decreasing the field. Inset: The magnetic effect shown in (a) after subtraction of the superconducting background, a function of the form $a|H| + b$. (d) Schematic illustration of adjacent domain orientation in the various resistance states. The data are taken from (b).

in all field orientations eliminates the anisotropic magneto-resistance as an explanation for the effect. In the GMR scenario the low resistance state appears when the domains are aligned while the high resistance state appears when the domains are not aligned. This interpretation of our results is schematically depicted in Fig. 3(d). The saturation field H_s is determined as the onset of the low resistance state.

We note the hysteretic behavior of resistance in all three field directions. Such hysteretic behavior is expected for magnetic field applied along an easy axis [24]. Vortices pinned to superconducting regions cannot be at the origin of the hysteresis since it is observed for the parallel field orientation where vortices do not exist. We can therefore conclude that the magnetization tends to align in the plane or along the crystal principle axis. A conspicuous difference between the in-plane and perpendicular field orientations is the abrupt transition from the high resistance to the low resistance states for the parallel direction. This suggests that the magnetic moment is pinned in the plane with a characteristic energy corresponding to a field of ≈ 100 G. Furthermore, a careful examination of our curves shows that the resistance returns to its zero field value before the magnetic field changes its direction (before reaching zero field). This is indicative of a nontrivial magnetic ground state with magnetic domains aligned antiparallel.

Figure 4 shows the resistance versus magnetic field for various orientations. We use these data to determine the angular dependence of H_s , which is plotted in Fig. 4(b). As expected, there is strong anisotropy between parallel and perpendicular field orientations. The anisotropy between parallel and transverse field directions strongly suggests that the magnetic effects come from the conducting region (the nanowire). It is important to note that application of gate voltage between -10 and 50 V did not change the saturation field in either the perpendicular configuration nor in the transverse one. This result is in line with gate independent magnetization found by Kalisky *et al.* [25].

In the inset of Fig. 5(a) we show the resistance versus magnetic field applied parallel to the nanowire. The saturation field H_s is determined for each temperature. We plot the saturation field as a function of temperature for both parallel and perpendicular directions. The data was fit to $H_s(T) = H_s(0)(1 - (T/T_0))^{1/2}$ for both orientations, with $H_s(0)$ as the saturation field at zero temperature. As expected, $H_s(0)$ is larger for parallel field orientation compared to the perpendicular one. The fit to the saturation field extrapolates to zero at the same temperature for both orientations within the error bar.

In Fig. 5(b) we show the normalized saturation field $H_s(T)/H_s(0)$ with $H_s(0)$ being the extrapolation to zero temperature (one could use the value at 20 mK with no significant difference). Both data sets collapse on the same curve. Assuming that the saturation field is proportional to the magnetization, fitting the data with $(1 - (T/T_{\text{Curie}}))^{1/2}$ should allow us to determine the Curie temperature to be $T_{\text{Curie}} = 954 \pm 20$ mK.

We note that resistance in the superconducting state is not zero [Fig. 2(a)]. The remnant resistance is tunable by gate voltage and is a significant fraction of the normal state

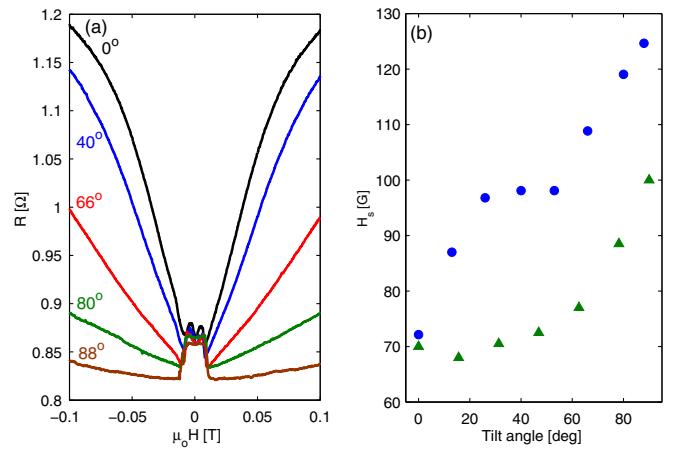


FIG. 4 (color online). (a) Resistance versus magnetic field for various angles between the perpendicular to the interface and the applied magnetic field 90 deg corresponds to the parallel field direction. (b) Saturation field for various angles. For the circles (triangles) 90 deg corresponds to the parallel (transverse) field orientation.

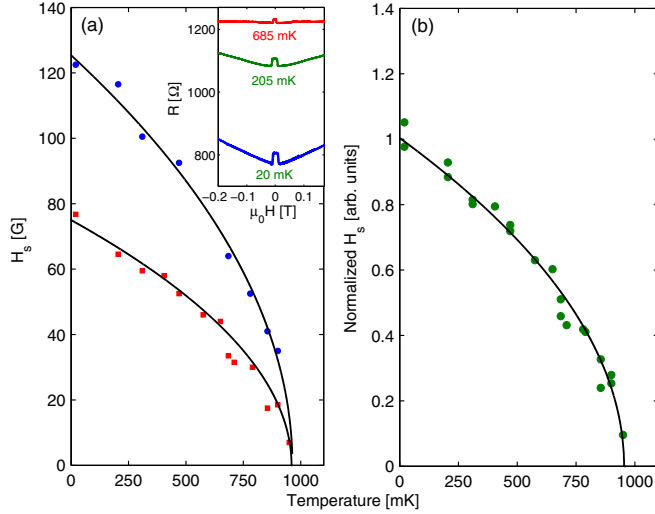


FIG. 5 (color online). Inset: Resistance versus magnetic field for various temperatures for parallel field orientation. (a) Saturation field H_s as a function of temperature for parallel and perpendicular field orientations. The solid lines are fits to $H_s(0)(1 - T/T_0)^{1/2}$. (b) Normalized saturation field $H_s(T)/H_s(0)$ for both parallel and perpendicular orientations. $H_s(0)$ is determined from the fit in (a). Black solid line is a fit to $(1 - T/T_{\text{Curie}})^{1/2}$ yielding $T_{\text{Curie}} = 954 \pm 20$ mK.

value. Assuming that the sheet resistance of the nanowire for various gate voltages has similar values compared to that obtained for larger samples, it follows that the contact resistance is relatively small. Hence, the residual resistance is not dominated by the contact. Finite residual resistance could arise from phase slips [26] due to the wire being narrower than the superconducting coherence length, $\xi \approx 100$ nm [22]. In order to find out the contribution of this mechanism, one should study the critical exponents of the low temperature resistivity; however, in our case it is masked by the magnetic effects. Another possibility is phase separation between magnetic regions and superconducting ones.

We believe that the low magnetic field effects are observable in our nanowires due to their small dimensions. This is in contrast to larger samples where the magnetic regions are shunted by low resistance, nonmagnetic paths. In our nanowires the current is forced through a series of magnetic resistors as well as through the nonmagnetic (superconducting at low temperature) ones. Making the sample smaller than the magnetic domain allows us to set a lower limit of 50 nm (sample width) on the magnetic patch size.

For field applied perpendicular to the interface [see Fig. 2(c)], one expects the magnetoresistance to be smaller in the nanowires due to the confinement, as observed. In addition, due to the confinement, which is not very far from the quantum limit, the phase space available for back-scattering is expected to be reduced [27]. We also note that the onset field for the SdH effect [see Fig. 2(c)] is similar to that observed in larger samples [21]. It is possible that the

SdH scattering rate (inverse Dingle time) is more sensitive to small angle scattering, which does not manifest itself in the resistivity.

Various probes agree on the existence of magnetism in the $\text{SrTiO}_3/\text{LaAlO}_3$ interface, but the details of the magnetic properties are still a matter of debate. Local scanning SQUID measurements, performed without the application of an external magnetic field, report the existence of randomly oriented local magnetic dipoles on the sample surface, resulting in zero or very small net magnetization over the whole sample [6]. On the other hand, torque magnetometry measurements, performed while applying an external magnetic field, revealed a nonzero sample magnetization [8] up to room temperature. Anisotropic magnetoresistance effects were reported to persist up to a temperature of 35 K [2] [4]. These experiments were performed at high magnetic fields, of the order of 10 T, sufficient to align all spins. A similar temperature scale was also reported by the β NMR study [9]. It is, however, possible that while free magnetic moments do exist up to higher temperatures, the magnetic order reported here forms only at lower temperatures. This view is also consistent with the absence of global magnetization observed down to 1.7 K [28]. Our experiment, therefore, provides the first direct indications for a nontrivial magnetic ground state at the interface, which vanishes above $T_{\text{Curie}} = 954 \pm 20$ mK.

Finally, we would like to address the question of whether superconductivity and magnetism coexist. In our case T_{Curie} is of the same order as the superconducting critical temperature T_c . This is a rare situation where superconductivity and magnetism can coexist. However, it is also possible that the reproducible features we observe are due to magnetic (nonsuperconducting) patches [6] connected in series to superconducting (nonmagnetic) regions, which are spatially separated. These patches cannot be bypassed by the electric current due to the small dimensions of the bridges making magnetism visible to transport. Our experiment cannot distinguish between these two scenarios.

In summary, we designed a unique method to fabricate nanowires from the $\text{SrTiO}_3/\text{LaAlO}_3$ interface. We measured transport through such 50 nm wide bridges. The Shubnikov–de Haas signal suggests that the wires have similar carrier concentration as the 2D system. For such low channel widths magnetic effects in the form of GMR become visible. This GMR is found to be independent of gate voltage within the range studied. From the hysteretic behavior of resistance versus magnetic field, we conclude that the moments tend to align in the plane or parallel to the crystal axis. We find that the underlying magnetic order is not simple ferromagnetic but one with antiparallel magnetic domains. From the temperature dependence of the saturation field, we find a Curie temperature of 954 ± 20 mK of the same order as the superconducting transition temperature.

We thank A. Segal, A. Palevski, A. Gerber, and N. Bachar for useful discussions. We give special thanks to Glover E. Jones for help in the magnet lab. This work was supported in part by the Israeli Science Foundation under Grant No. 569/13 by the Ministry of Science and Technology under Contract No. 3-8667 and by the U.S.-Israel Binational Science Foundation (BSF) under Grant No. 2010140. A portion of this work was performed at the National High Magnetic Field Laboratory, which is supported by National Science Foundation Cooperative Agreement No. DMR-0654118, the State of Florida, and the U.S. Department of Energy. J.-H. P. and D. G. acknowledge support from the U.S. Department of Energy (DOE) from Grant No. DOE NNSA DE-NA0001979.

*yodagan@post.tau.ac.il

- [1] A. Brinkman, M. Huijben, M. Van Zalk, J. Huijben, U. Zeitler, J. Maan, W. Van der Wiel, G. Rijnders, D. Blank, and H. Hilgenkamp, *Nat. Mater.* **6**, 493 (2007).
- [2] M. Ben Shalom, C. W. Tai, Y. S. Lereah, M. Sachs, E. Levy, D. Rakhmilevitch, A. Palevski, and Y. Dagan, *Phys. Rev. B* **80**, 140403 (2009).
- [3] S. Seri and L. Klein, *Phys. Rev. B* **80**, 180410 (2009).
- [4] E. Flekser, M. Ben Shalom, M. Kim, C. Bell, Y. Hikita, H. Y. Hwang, and Y. Dagan, *Phys. Rev. B* **86**, 121104 (2012).
- [5] G. Cheng, J. P. Veazey, P. Irvin, C. Cen, D. F. Bogorin, F. Bi, M. Huang, S. Lu, C.-W. Bark, S. Ryu *et al.*, *Phys. Rev. X* **3**, 011021 (2013).
- [6] J. A. Bert, B. Kalisky, C. Bell, M. Kim, Y. Hikita, H. Y. Hwang, and K. A. Moler, *Nat. Phys.* **7**, 767 (2011).
- [7] D. A. Dikin, M. Mehta, C. W. Bark, C. M. Folkman, C. B. Eom, and V. Chandrasekhar, *Phys. Rev. Lett.* **107**, 056802 (2011).
- [8] L. Li, C. Richter, J. Mannhart, and R. Ashoori, *Nat. Phys.* **7**, 762 (2011).
- [9] Z. Salman, O. Ofer, M. Radovic, H. Hao, M. Ben Shalom, K. H. Chow, Y. Dagan, M. D. Hossain, C. D. P. Levy, W. A. MacFarlane *et al.*, *Phys. Rev. Lett.* **109**, 257207 (2012).
- [10] J.-S. Lee, Y. Xie, H. Sato, C. Bell, Y. Hikita, H. Hwang, and C.-C. Kao, *Nat. Mater.* **12**, 703 (2013).
- [11] A. Ron and Y. Dagan, *Phys. Rev. Lett.* **112**, 136801 (2014).
- [12] K. Michaeli, A. C. Potter, and P. A. Lee, *Phys. Rev. Lett.* **108**, 117003 (2012).
- [13] S. Banerjee, O. Erten, and M. Randeria, *Nat. Phys.* **9**, 626 (2013).
- [14] J. Ruhman, A. Joshua, S. Ilani, and E. Altman, *Phys. Rev. B* **90**, 125123 (2014).
- [15] D. Rakhmilevitch, M. Ben Shalom, M. Eshkol, A. Tsukernik, A. Palevski, and Y. Dagan, *Phys. Rev. B* **82**, 235119 (2010).
- [16] D. Stornaiuolo, S. Gariglio, N. J. G. Couto, A. Fte, A. D. Caviglia, G. Seyfarth, D. Jaccard, A. F. Morpurgo, and J.-M. Triscone, *Appl. Phys. Lett.* **101**, 222601 (2012).
- [17] J.-W. Chang, J. Song, J. S. Lee, H. Noh, S. K. Seung, L. Baasandorj, S. G. Lee, Y.-J. Doh, and J. Kim, *Appl. Phys. Express* **6**, 085201 (2013).
- [18] A. Kalabukhov, R. Gunnarsson, J. Börjesson, E. Olsson, T. Claesson, and D. Winkler, *Phys. Rev. B* **75**, 121404 (2007).
- [19] M. Salluzzo, S. Gariglio, D. Stornaiuolo, V. Sessi, S. Rusponi, C. Piamonteze, G. M. De Luca, M. Minola, D. Marré, A. Gadaleta *et al.*, *Phys. Rev. Lett.* **111**, 087204 (2013).
- [20] I. Sternfeld, E. Levy, M. Eshkol, A. Tsukernik, M. Karpovskii, H. Shtrikman, A. Kretinin, and A. Palevski, *Phys. Rev. Lett.* **107**, 037001 (2011).
- [21] M. Ben Shalom, A. Ron, A. Palevski, and Y. Dagan, *Phys. Rev. Lett.* **105**, 206401 (2010).
- [22] M. Ben Shalom, M. Sachs, D. Rakhmilevitch, A. Palevski, and Y. Dagan, *Phys. Rev. Lett.* **104**, 126802 (2010).
- [23] C. Chien, J. Q. Xiao, and J. S. Jiang, *J. Appl. Phys.* **73**, 5309 (1993).
- [24] E. C. Stoner and E. Wohlfarth, *Phil. Trans. R. Soc. A* **240**, 599 (1948).
- [25] B. Kalisky, J. A. Bert, B. B. Klopfer, C. Bell, H. K. Sato, M. Hosoda, Y. Hikita, H. Y. Hwang, and K. A. Moler, *Nat. Commun.* **3**, 922 (2012).
- [26] A. Bezryadin, C. Lau, and M. Tinkham, *Nature (London)* **404**, 971 (2000).
- [27] H. Sakaki, *Jpn. J. Appl. Phys.* **19**, L735 (1980).
- [28] M. R. Fitzsimmons, N. W. Hengartner, S. Singh, M. Zhernenkov, F. Y. Bruno, J. Santamaria, A. Brinkman, M. Huijben, H. J. A. Molegraaf, J. de la Venta *et al.*, *Phys. Rev. Lett.* **107**, 217201 (2011).